GROUPED SPARSITY ALGORITHM FOR MULTICHANNEL INTRACARDIAC ECG SYNCHRONIZATION

T. Trigano, V. Kolesnikov*, D. Luengo†, A. Artés-Rodríguez‡*

* Dep. of Electrical Engineering, Shamoon College of Engineering, Ashdod, Israel
† Dep. of Circuits and Sytems Engineering, Univ. Politécnica de Madrid, Madrid, Spain
‡ Dep. of Signal Theory and Communications, Univ. Carlos III de Madrid, Leganés, Spain

ABSTRACT

In this paper, a new method is presented to ensure automatic synchronization of intracardiac ECG data, yielding a three-stage algorithm. We first compute a robust estimate of the derivative of the data to remove low-frequency perturbations. Then we provide a grouped-sparse representation of the data, by means of the Group LASSO, to ensure that all the electrical spikes are simultaneously detected. Finally, a post-processing step, based on a variance analysis, is performed to discard false alarms. Preliminary results on real data for sinus rhythm and atrial fibrillation show the potential of this approach.

1. INTRODUCTION

Digital signal processing techniques have been extensively used in the analysis of biomedical signals. Historically, electrocardiograms (ECGs) were among the first signals to be processed, and nowadays are routinely used in diagnosis, therapy and monitoring situations [1]. Here we focus on the analysis of multi-channel intracardiac ECGs, also known as electrograms (EGMs). Intracardiac ECGs are used in implantable devices (e.g., pacemakers and defibrillators) for several applications: identification of ventricular tachycardias [2], early alert of the presence of acute myocardial infarction [3], arrhythmia classification for appropriate therapy delivery [4], etc. EGMs are also acquired during heart surgery performed on patients with sustained atrial fibrillation (AF), which is one of the most common heart disorders, to guide catheter ablation for patients not responding to drug therapies [5].

The analysis of EGMs has been traditionally based on single-channel frequency [6] or time-frequency approaches [7]. Alternative methods, based on organization analysis and its combination with frequency analysis have also been considered [8]. More recently, machine learning techniques (e.g., support vector machines [4]) and sparse learning/inference schemes [9–11] have also been introduced. However, all of these methods are still typically based on a channel-by-channel approach, and EGM signals suffer from many distortions (such as baseline wander, breath-induced amplitude modulation or severe noise and interference [1]), which may prevent the detection of some activations in one or more channels. A multi-channel approach, which takes into account the information from all the channels simultaneously, will help to alleviate this losses, thus adding robustness to any further signal processing stage based on the detected spikes.

In this paper, a new method is presented to ensure automatic synchronization of multiple EGM channels, yielding a three-stage algorithm. A robust estimate of the derivative of the data is computed first to remove low-frequency perturbations. This is followed by a joint sparse representation of the data, based on the Group LASSO, to ensure that the electrical spikes corresponding to all the channels are simultaneously detected. Finally, a post-processing step, based on a variance analysis, is performed to discard false alarms. The resulting algorithm is a multi-channel extension of the single-channel sparse spike inference approach developed in [9]. Preliminary results obtained on real data, both for sinus rhythm and atrial fibrillation, show the potential of this approach.

2. SYNCHRONOUS SPIKE DETECTION FROM INTRACARDIAC ECG DATA

2.1. Model Description

Assume that we observe a multichannel signal stemming, in our case, from intracardiac ECG measurements, uniformly sampled with sampling period T_s. This discrete signal can be modelled by a matrix $\mathbf{Y}$ of size $N \times Q$, where Q denotes the number of channels (i.e., the number of electrodes) and N denotes the number of sampling points recorded:

$$\mathbf{Y} \triangleq \begin{bmatrix} y_1[0] & y_2[0] & \cdots & y_Q[0] \\ y_1[1] & y_2[1] & \cdots & y_Q[1] \\ \vdots & \vdots & \ddots & \vdots \\ y_1[N-1] & y_2[N-1] & \cdots & y_Q[N-1] \end{bmatrix} . \quad (1)$$

This work has been funded by the Spanish government's projects COMONSENS (CSD2008-00010), ALCIT (TEC2012-38800-C03-01), COMPREHENSION (TEC2012-38883-C02-01) and DISSECT (TEC2012-38058-C03-01).

Each signal $y_q[n]$ consists mainly of localized pulses, characterizing the heart activity, and a slowly varying baseline, also known as *baseline wander* (see e.g. [1]). Hence, a first preliminary step is required before further analysis, namely a baseline removal. A basic differentiation would magnify the recorded perturbations (noise, powerline interference, etc. [1]). Therefore, a more robust estimate of the signal derivative is described in the following section.

2.2. Robust derivative estimation for data analysis

The estimation of a functional derivative is a well known problem in the statistical community. In this paper, we apply the robust method described in [12] to approximate the signal's empirical derivative by means of the weighted average of a collection of difference quotients,

$$z_j[n] = \sum_{i=1}^{k} w_i \frac{y_j[n+i] - y_j[n-i]}{2iT_s}, \tag{2}$$

where k is a tuning parameter that controls the smoothness of the curve obtained, and the weights w_j are chosen as

$$w_j = \frac{6j^2}{k(k+1)(2k+1)}$$

in order to minimize the variance of (2), as proved in [12, Proposition 1]. The latter procedure provides a clean derivative estimate, in the sense that the baseline is suppressed and the influence of noisy artifacts is significantly reduced, as seen in Figure 1 for $k = 12$. This comes at the price of an increased bias in the estimation of the true derivative, which increases as k grows. However, it is important to remark that we are not interested in a perfect reconstruction, but rather on partial information, which is pulse localization. As in Eq. (1), we shall denote by $\mathbf{Z}$ the matrix of signal derivatives, $z_q[n]$ for $q = 1, \ldots, Q$ and $n = 0, \ldots, N-1$.

2.3. Grouped-sparsity representation for spike detection

Our next step is providing a sparse representation of $\mathbf{Z}$ by means of a pre-defined dictionary $\mathbf{A}$, in order to estimate the pulse arrivals simultaneously in all channels. Note again that we are only interested in the localization of the pulses, not in the full representation of the observed signals, and that no optimal base is known for the ECG signal representation. Therefore, the chosen dictionary must be *time-structured* and *overcomplete*, in the sense that the same collection of basic shapes has to be associated to each sampling point, since we cannot predict neither the exact occurrences of electrical pulses nor their shape.

Mathematically, if we assume that the signals are created from M discretized basis waveforms, $a_m[n] = a_m(nT_s) \neq 0 \Leftrightarrow -N_m \leq n \leq N_m$ for $m = 1, \ldots, M$, then

$$\mathbf{A} = [\mathbf{A}_0 \; \mathbf{A}_1 \; \cdots \; \mathbf{A}_{N-1}]$$

is an $N \times MN$ overcomplete dictionary, with $M > 1$ indicating the number of basis signals in the dictionary and $\mathbf{A}_\ell = [\mathbf{a}_{1,\ell}, \ldots, \mathbf{a}_{M,\ell}]$ being the ℓ-th $N \times M$ circulant dictionary matrix, with $\mathbf{a}_{m,\ell} = [a_m[-\ell], \ldots, a_m[-1], a_m[0], a_m[1], \ldots, a_m[N-1-\ell]]^\top$ the $N \times 1$ vector corresponding to the m-th basis waveform shifted to $n = \ell$. Now, let us denote by $\mathbf{s}$ the $NQ \times 1$ vector obtained concatenating the columns of $\mathbf{Z}$, i.e.,

$$\mathbf{s} \triangleq [\mathbf{z}_1^\top, \; \mathbf{z}_2^\top, \; \ldots, \; \mathbf{z}_Q^\top]^\top, \tag{3}$$

with $\mathbf{z}_q^\top = [z_q[0], \ldots, z_q[N-1]]$ $(1 \leq q \leq Q)$, and by $\mathbf{B}$ the $NQ \times MNQ$ block diagonal matrix obtained replicating $\mathbf{A}$:

$$\mathbf{B} \triangleq \begin{bmatrix} \mathbf{A} & \mathbf{0} & \cdots & \mathbf{0} \\ \mathbf{0} & \mathbf{A} & \cdots & \mathbf{0} \\ \vdots & \vdots & \ddots & \vdots \\ \mathbf{0} & \mathbf{0} & \cdots & \mathbf{A} \end{bmatrix}. \tag{4}$$

Assuming a sparse decomposition of $\mathbf{s}$ according to $\mathbf{B}$, our reconstruction model is

$$\mathbf{s} = \mathbf{B}\boldsymbol{\beta} + \boldsymbol{\varepsilon},$$

where $\boldsymbol{\beta}$ is the $MNQ \times 1$ vector containing the decomposition of $\mathbf{s}$ according to the dictionary $\mathbf{B}$ and $\boldsymbol{\varepsilon}$ is the $NQ \times 1$ additive white Gaussian noise vector.

When the channels are perfectly synchronized, $\boldsymbol{\beta}$ can be decomposed into groups of coefficients being active or inactive altogether. Let us denote by G the integer set $G \triangleq \{1, 2, \ldots, MNQ\}$ of column indices of $\mathbf{B}$, and define the subsets

$$G_n \triangleq \{m + nM + (q-1)MN, \; 1 \leq m \leq M, 1 \leq q \leq Q\}, \tag{5}$$

for $n = 0, \ldots, N-1$. From (5), it is clear that the G_n form a partition of G, i.e., $G = \cup_{n=0}^{N-1} G_n$ with $G_n \neq \emptyset$ and $G_\ell \cap G_n = \emptyset$ for any $\ell \neq n$ with $\ell, n \in \{0, \ldots, N-1\}$. Similarly, for any vector $\boldsymbol{\beta} = [\beta_1, \beta_2, \ldots, \beta_{MNP}]^\top$ we denote by $\boldsymbol{\beta}_{G_n}$ the vector whose coefficients are equal to β_p if $p \in G_n$ and 0 otherwise. Following (4) and (5), the Group LASSO solution is given by [13]

$$\widehat{\boldsymbol{\beta}} = \underset{\boldsymbol{\beta} \in \mathbb{R}^{MNQ}}{\arg\min} \; \|\mathbf{s} - \mathbf{B}\boldsymbol{\beta}\|_2^2 + \lambda \sum_{n=0}^{N-1} \|\boldsymbol{\beta}_{G_n}\|_2, \tag{6}$$

where λ is a user-defined parameter quantifying the level of desired block-sparsity. Note that the subsets G_n are defined in such a way that $\boldsymbol{\beta}_{G_n}$ contains all the coefficients for the sparse decomposition, at the time instant n, of all the channels ($z_q[n]$ for $q = 1, \ldots, Q$) using all the waveforms in the dictionary ($a_m[n]$ for $m = 1, \ldots, M$).

Eq. (6) is of interest if we aim to keep synchronicity between channels. In a nutshell, it enforces grouped sparsity

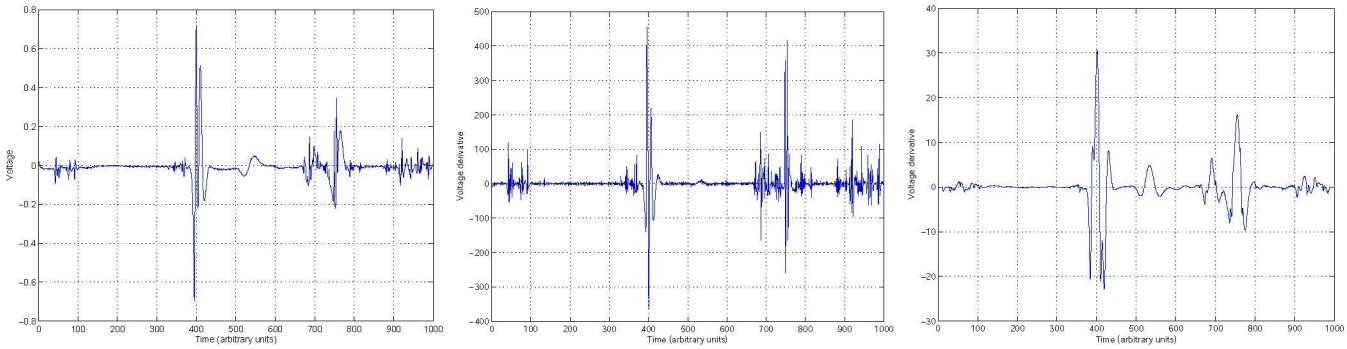

Fig. 1. Original signal (left), standard derivative (center), estimate from (2) using $k = 12$ (right)

instead of coefficient driven sparsity, and it can be proved that all the coefficients within a group contribute to the regression whenever it is active [13]. Hence, if the groups are created according to (5), the coefficients related to similar starting points of different channels would be active/inactive altogether. In a sense, we could say that the group LASSO described in (6) forces synchronicity between channels, enforcing a pulse localization in the same neighborhood of the other channels whenever we detect a pulse in one channel. Note, however, that the dictionary used is not ideal, as the real pulse shapes are unknown. Therefore, false localizations may occur, and the coefficients obtained in (6) must be post-processed in order to obtain a robust estimate of the arrival times of the pulses.

2.4. Post-processing and arrival times estimation

We recall that the observed array of signals is not created using the chosen dictionary $\mathbf{B}$. Indeed, the shape of the observed pulses can change substantially from one channel to another and may also be slowly time-varying. Consequently, it is likely that an individual pulse on one channel will not be estimated with a single given shape a_m, but rather by a combination of shapes found in consecutive subdictionaries $\mathbf{A}_\ell$. This fact can become an issue if our aim is estimating the pulse arrival times. In order to solve this problem, we introduce a post-processing step adapted to the Group LASSO particularities.

If a group of variables is active, it could either represent an actual electrical pulse or a segment of noise (either additive, either stemming from the differentiation step). We suggest in this paper the following post-processing of $\widehat{\boldsymbol{\beta}}$. For each group G_n, we set

$$\widehat{\boldsymbol{\beta}}_{G_n}^{new} = \begin{cases} \widehat{\boldsymbol{\beta}}_{G_n}, & \mathrm{Var}(\widehat{\boldsymbol{\beta}}_{G_n}) > \sigma_G^2; \\ 0, & \text{otherwise}; \end{cases} \quad (7)$$

where $\mathrm{Var}(\widehat{\boldsymbol{\beta}}_{G_n})$ denotes the empirical variance of the coefficients of the group G_n, and σ_G^2 is a user-defined threshold (the choice of its value is discussed in the results section).

The motivation for (7) stems from our non-ideal choice of the dictionary. Since $\mathbf{B}$ only approximates the recorded ECG, it is likely that, when a pulse occurs, the group LASSO will activate several consecutive groups to provide a good regressor, and that a few coefficients inside the groups will represent the main waveform, whereas the remaining coefficients will be much smaller and just serve to refine the regression. On the other hand, when the group LASSO provides active groups to estimate the additive noise, all coefficients will have the same order of magnitude. These considerations make the variance of the coefficients of the active groups a valid numerical choice to distinguish between noise and actual pulses. Ideally, for pure noise the groups should be inactive, thus providing a variance equal to 0, which is consistent with our choice. Moreover, we assume that all successive active groups are related to the same electrical pulse, and estimate the number of electrical pulses and their locations iteratively as

$$t_n = \min\{\ell > t_{n-1} \ : \ \|\widehat{\boldsymbol{\beta}}_{G_{\ell-1}}^{new}\|_2 = 0, \|\widehat{\boldsymbol{\beta}}_{G_\ell}^{new}\|_2 > 0\}. \quad (8)$$

Signal to Noise Ratio

3. RESULTS

We present in this section results obtained on real ECG data provided by Dr. Angel Arenas' team from Madrid's Gregorio Marañón hospital (Spain). The signals correspond to patients with sustained atrial fibrillation (AF) and were obtained during heart surgery. They can be divided into two groups: artificially induced sinus rhythm and AF signals. All of the recordings were performed using a lasso catheter, which provides $Q = 10$ bipolar intracardiac ECGs (i.e., channels) with sampling frequency $f_s = 1/T_s = 977$ Hz.

3.1. Experimental settings

Since the true shape of the pulses is unknown, in this contribution we use a smooth dictionary $\mathbf{B}$ composed of truncated

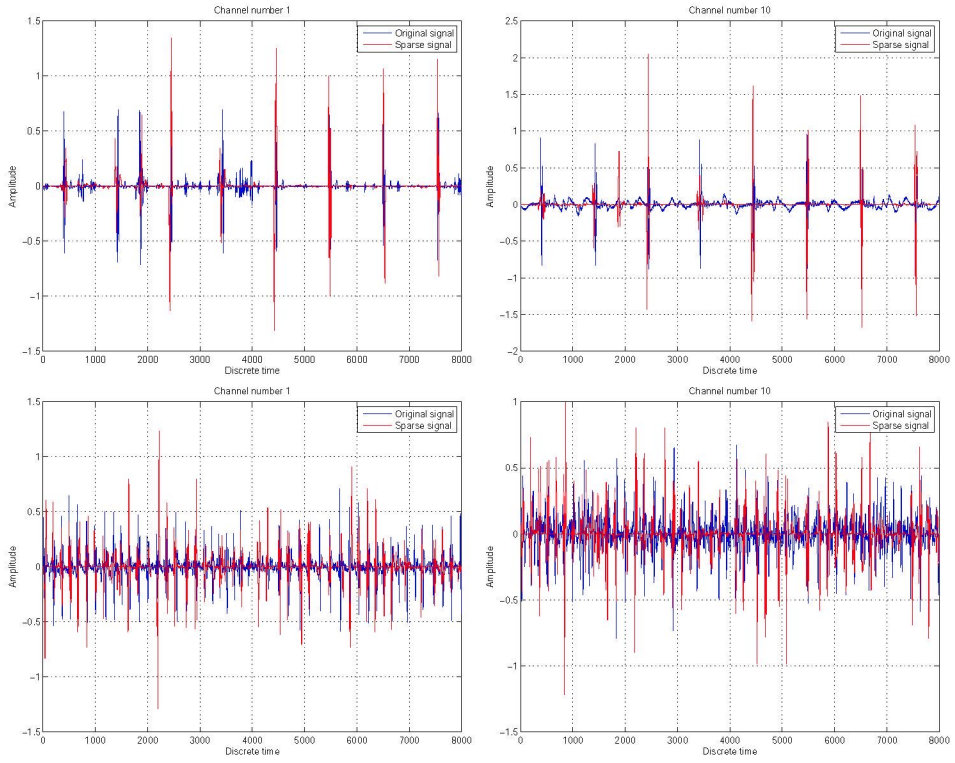

Fig. 2. Signal derivatives (blue) and sparse approximations (red) of channel 1 and 10 of the recordings for sinusal data (above) and atrial fibrillation (below).

Gaussian shapes, i.e.,

$$a_m[n] = e^{-n^2/2\sigma_m^2}, \quad n = -15, \ \ldots, \ 15,$$

where $\sigma_m \in \{1, 2, 3, 4, 5, 6\}$. The number of points used in (2) is chosen so that $k = 6$, which has been shown experimentally to provide a reasonable bias-variance tradeoff in our dataset. The parameters in the sparse inference algorithm were also obtained empirically through an extensive grid search over several scales. The sparsity parameter in (6) was set to $\lambda = 0.002$ for sinusal data and $\lambda = 0.0005$ for atrial fibrillation, and we found in both cases that setting $\sigma_G^2 = 0.0002$ in (7) was a good choice. The optimization is performed by using a thresholded-gradient method known as the FISTA method [14]. Since the proposed algorithm involves matrices of high dimensions, we split the signals in blocks of 80 sample times and perform the analysis on each block separately. Though the signal could be split in the middle of an electrical pulse, the post-processing allows us to solve this issue.

3.2. Results and discussion

Figure 2 presents two channels and their sparse approximations by means of the proposed approach, both for sinus rhythm and AF. We can see that, provided the sparsity parameters are well suited, the peaks of the ECG recordings can be easily detected, and most of the spurious signals and noise removed. Moreover, the synchronous reconstruction enables us to detect peaks even on channels with lower Signal to Noise Ratio, which is a significant advantage. An example of the estimated arrival times for sinus rhythm is presented in Fig. 3. The observation of these two figures illustrates both the advantages and shortcomings of the proposed approach. On the one hand, it can be observed that the pulse arrivals are well detected and synchronous, which is typical of sinus rhythm. In this sense, the algorithm will yield a more precise frequency analysis and improve the approaches of [9, 10]. On the other hand, when one abnormal pulse is detected (as in the first channel), the false detection will appear in all the channels (e.g., in channel 10 around sample time 2000). For AF, it is difficult to distinguish normal pulses from outliers, as the ground truth is unknown. However, we note that synchronization has also been achieved and a great deal of distortion removed from the signals (see channel 10 in Fig. 2). Note that these issues are strongly related to a post-processing step, since $\mathbf{B}_k$ is made of several columns which characterizes pulses starting at the same time. Indeed, it is important to remark that both the robust derivative estimator introduced in the pre-processing stage and the novel post-processing of the group LASSO results (based on the intra-group coefficient variance) are crucial to attain the results shown in Figs. 2 and 3. Finally, let us remark that the proposed approach

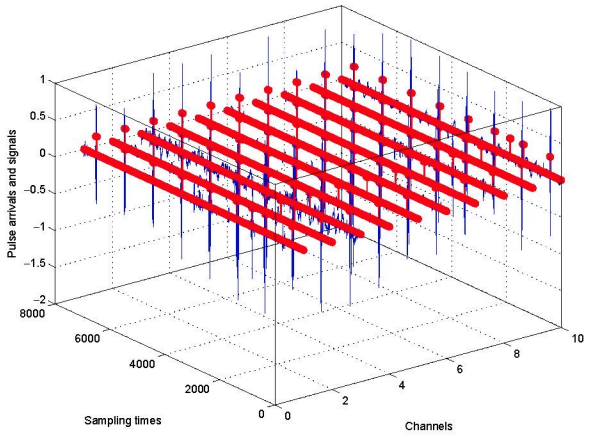

Fig. 3. Estimated times of all the channels and the associated signals. The estimated times are well synchronized, and most of the noisy parts are removed.

does not take into account neither the refractory period nor the refinement of [10], which we plan to introduce in future works.

4. CONCLUSION

We have presented an efficient way to detect ECG pulses simultaneously from multichannel recordings based on the well-known group LASSO approach. The preliminary robust estimation of the derivative allows us to significantly reduce the noise influence, whereas the novel post-processing introduced allows us to eliminate false alarms in the group LASSO representation. A more extensive investigation of the performance of the proposed method on atrial fibrillation datasets, the addition of regularization terms taking into account the physical constraints of the heart electrical activity, and more sophisticated and flexible multi-channel approaches (e.g., group LASSO with overlapping groups or social sparsity approaches) will be investigated in future contributions.

REFERENCES

[1] L. Sörnmo and P. Laguna, *Bioelectrical Signal Processing in Cardiac and Neurological Applications*, Academic Press, Jun. 2005.

[2] K. Yoshida *et al.*, "The value of defibrillator electrograms for recognition of clinical ventricular tachycardias and for pace mapping of post-infarction ventricular tachycardia," *Journal of the American College of Cardiology*, vol. 56, no. 12, pp. 970–979, 2010.

[3] T. A. Fischell *et al.*, "Initial clinical results using intracardiac electrogram monitoring to detect and alert patients during coronary plaque rupture and ischemia," *Journal of the American College of Cardiology*, vol. 56, no. 14, pp. 1089–1098, 2010.

[4] P. Milpied *et al.*, "Arrhythmia discrimination in implantable cardioverter defibrillators using support vector machines applied to a new representation of electrograms," *IEEE Transactions on Biomedical Engineering*, vol. 58, no. 6, pp. 1797–1803, June 2011.

[5] M. Wright *et al.*, "State of the art: Catheter ablation of atrial fibrillation," *Journal of Cardiovascular Electrophysiology*, vol. 19, no. 6, pp. 583–592, June 2008.

[6] Gerald Fischer *et al.*, "On computing dominant frequency from bipolar intracardiac electrograms," *IEEE Transactions on Biomedical Engineering*, vol. 54, no. 1, pp. 165–169, Jan. 2007.

[7] M. Stridh, L. Sörnmo, C. J. Meurling, and S. B. Olsson, "Sequential characterization of atrial tachyarrhythmias based on ECG time-frequency analysis," *IEEE Transactions on Biomedical Engineering*, vol. 51, no. 1, pp. 100–114, Jan. 2004.

[8] O. Barquero-Pérez *et al.*, "Fundamental frequency and regularity of cardiac electrograms with Fourier organization analysis.," *IEEE Transactions on Biomedical Engineering*, vol. 57, no. 9, pp. 2168–2177, 2010.

[9] S. Monzón, T. Trigano, D. Luengo, and A. Artés-Rodríguez, "Sparse Spectral Analysis of Atrial Fibrillation Electrograms," in *Proc. IEEE Int. Wkshp. on Machine Learning for Signal Processing (MLSP)*, Sep. 2012, pp. 1–6.

[10] D. Luengo, J. Vía, S. Monzón, T. Trigano, and A. Artés-Rodríguez, "Cross-products LASSO," in *Proc. IEEE Int. Conf. on Acoustics, Speech and Signal Processing (ICASSP)*, May 2013, pp. 6118–6122.

[11] U. Richter, *Spatial Characterization and Estimation of Intracardiac Propagation Patterns During Atrial Fibrillation*, Ph.D. thesis, Lund University, 2010.

[12] K. De Brabanter, J. De Brabanter, B. De Moor, and I. Gijbels, "Derivative estimation with local polynomial fitting," *Journal of Machine Learning Research*, vol. 14, pp. 281–301, Jan. 2013.

[13] M. Yuan and Y. Lin, "Model Selection and Estimation in Regression with Grouped Variables," *Journal of the Royal Statistical Society: Series B (Statistical Methodology)*, vol. 68, no. 1, pp. 49–67, 2006.

[14] A. Beck and M. Teboulle, "A fast iterative shrinkage-thresholding algorithm for linear inverse problems," *SIAM Journal on Imaging Sciences*, vol. 2, pp. 183–202, 2009.